

# New Insight into Antiproton Production and Reabsorption Using Proton-Nucleus Collisions at the AGS

Saskia Mioduszewski for the E910 Collaboration \*

Department of Physics, Building 510C, Brookhaven National Laboratory, Upton, NY 11973, USA

Antiproton ( $\bar{p}$ ) yields are presented for proton-nucleus collisions, with targets Be, Cu, and Au, at beam momenta of 12.3 and 17.5 GeV/c. In addition to target size and beam momentum, the number of projectile collisions  $\nu$ , as derived from the number of “grey” tracks (slow protons and deuterons), is used to disentangle the  $\bar{p}$  reabsorption from the production. By quantifying the amount of reabsorption of the  $\bar{p}$  within the nucleus as a function of  $\nu$ , the annihilation within the nucleus is estimated and compared to the free annihilation cross section. Preliminary results on antilambda ( $\bar{\Lambda}$ ) production as a function of  $\nu$  are also presented for comparison.

## 1. Introduction

Sub-threshold  $\bar{p}$  production as well as an apparently reduced  $p - \bar{p}$  annihilation cross section in the nucleus have been under debate since the discovery of the  $\bar{p}$  and until recently [1–8]. The observation of enhanced antimatter production has been proposed as a signature of the Quark Gluon Plasma [9]. Due to the annihilation of antibaryons in baryon-rich nuclear matter, it has also been proposed to use  $\bar{p}$  yields as a measure of the baryon density in heavy ion collisions [10]. These interesting prospects for using antibaryons to help determine the properties of the hot, dense phase in a heavy ion collision require a deeper understanding of both the production and reabsorption of the  $\bar{p}$  within the nucleus. Proton-nucleus collisions provide a cleaner environment for testing  $\bar{p}$  production and reabsorption within the nucleus than heavy ion collisions. In this paper, we present measurements of  $\bar{p}$  production in  $p+A$  collisions at the AGS that may help address the questions of production and reabsorption in the nucleus.

## 2. Data Reduction

The E910 apparatus has been described elsewhere [11]. The time-of-flight (TOF) wall, used to identify the  $\bar{p}$ , is located approximately 8 m from the target and covers approximately  $5 \times 2$  m<sup>2</sup>. Using the measured times of flight to identify particles, the  $\bar{p}$  band is

---

\*supported by US-DOE under contracts with BNL (DE-AC02-98CH10886), Columbia (DE-FG02-86ER40281), ISU (DE-FG02-92ER4069), KSU (DE-FG02-89ER40531), LBNL (DE-AC03-76F00098), LLNL (W-7405-ENG-48), ORNL (DE-AC05-96OR22464), and UT (DE-FG02-96ER40982) and NSF under contract with FSU (PHY-9523974).

well separated from the pions and kaons up to 3.5 GeV/c. Momentum dependent cuts on the number of standard deviations of the measured TOF from the expected TOF of a proton are applied. To reduce background in the identified  $\bar{p}$  sample, we apply cuts on the particle's ionization energy loss in the TPC and the measured photoelectrons in the Cerenkov detector. Quality cuts on the hits on the TOF include a cut on the difference in horizontal position between a projected track and the center of the hit TOF slat and a cut on the energy deposited on the TOF slat. Tracks are matched to the TOF wall with a  $90\pm 5\%$  efficiency. We estimate and subtract a momentum-dependent background of approximately 5%. Feeddown from  $\bar{\Lambda}$  in our  $\bar{p}$  sample is estimated to be less than 5%. The data have been acceptance corrected within our  $y - p_T$  coverage, and corrected for the efficiencies of the cuts mentioned above. All results are shown within our  $y - p_T$  coverage,  $y = (1, 2)$  and  $p_T = (10, 800)$  MeV/c.

### 3. Measured Antiproton Yields

The  $\bar{p}$  yields are shown in Fig. 1. We observe a strong increase in  $p$ +Au  $\bar{p}$  yields from beam momentum 12.3 to 17.5 GeV/c as expected, since production of  $\bar{p}$  near threshold should depend sensitively on the available phase space. Although the likelihood of producing a  $\bar{p}$  may be greater in a larger nucleus [12], the likelihood of reabsorption is also greater in the presence of more baryons. These two countervailing effects can be studied by investigating the target dependence of  $\bar{p}$  yields. Results for Be, Cu, and Au at beam momentum 12.3 GeV/c are also shown in Fig. 1.

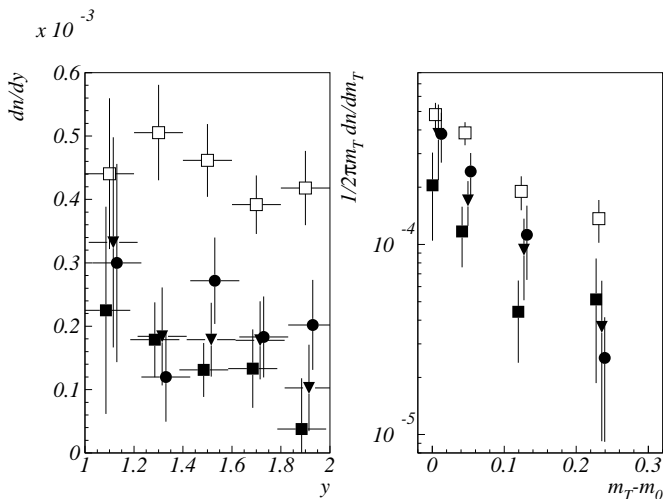


Figure 1. Beam momentum and target dependence of rapidity densities (left) and transverse mass densities (right). The open squares are 17.5 GeV/c  $p$ +Au yields, solid squares are 12.3 GeV/c  $p$ +Au, solid triangles are 12.3 GeV/c  $p$ +Cu, and solid circles are 12.3 GeV/c  $p$ +Be.

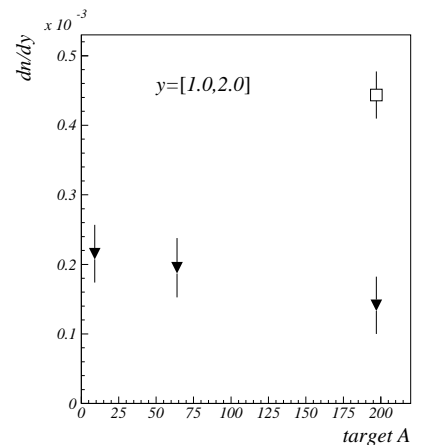


Figure 2. Integrated rapidity density as a function of target  $A$ . The triangles are yields from 12.3 GeV/c beam momentum, and the open square is 17.5 GeV/c.

Figure 2 shows the integrated rapidity densities for all four data sets. The yields decrease from  $p$ +Be to  $p$ +Au collisions by  $34 \pm 22\%$ .

#### 4. Reabsorption of the Antiprotons

By characterizing collision “centrality,” E910 can provide new insight into  $\bar{p}$  absorption. Events are characterized by the mean number of collisions  $\nu$  that the projectile undergoes within the nucleus (as determined by the number of “grey” tracks  $N_g$ ) [11]. The  $\nu$  dependence of the mean  $\bar{p}$  multiplicity in 17.5 GeV/c  $p$ +Au collisions is shown in Fig. 3. A preliminary measurement of the mean  $\bar{\Lambda}$  multiplicity as a function of  $\nu$  is also shown in Fig. 4. The mean multiplicity of both tends to decrease as  $\nu$  increases. Although not convincingly significant, the increase from  $N_g = 0$  to  $N_g = 1$  in the mean  $\bar{p}$  yield may be evident of a contribution to production beyond the first  $p$ +N collision. The increase is more pronounced in the mean  $\bar{\Lambda}$  yield versus  $\nu$  and thus strengthens the evidence for production beyond a first collision model. With the following assumptions, we quantify the “effective” absorption cross section in the nucleus and show that it is greatly reduced relative to the free  $p - \bar{p}$  annihilation cross section. The first assumption is that the  $\bar{p}$  is predominantly produced in the first  $p$ +N collision. Since the beam energy is near the production threshold, this is generally assumed to be true at AGS energies [13]. If there are contributions to production beyond  $\nu = 1$ , as we have conjectured, they are not large enough to change our conclusion dramatically. The second assumption is that the  $\bar{p}$  follows the path of the projectile through the nuclear matter. This is also a reasonable assumption because we observe strongly forward-peaked angular distributions for the  $\bar{p}$ . Then the survival probability of the  $\bar{p}$  can be described by the following equation (although one should note that a formation time is not taken into account by this description),

$$\sigma(pA \rightarrow \bar{p}X) = \sigma(pp \rightarrow \bar{p}X)e^{-\frac{\sigma_{abs}}{\sigma_{pN}}(\nu-1)}. \quad (1)$$

Since the value  $\nu$  plotted on the x-axis of Figs. 3 and 4 is simply an average value,  $\bar{\nu}(N_g)$ , and each value of  $N_g$  actually has a distribution of  $\nu$  values associated with it,  $P_{N_g}(\nu)$ , we fold the above exponential with  $P_{N_g}(\nu)$ . We determine  $\sigma_{abs}$  by fitting with,

$$\sigma(pA \rightarrow \bar{p}X) = \sigma(pp \rightarrow \bar{p}X)P_{N_g}(\nu)e^{-\frac{\sigma_{abs}}{\sigma_{pN}}(\nu-1)}. \quad (2)$$

In one fit, the first data point is not included (because of the initial increase in yield from  $N_g = 0$  to  $N_g = 1$ ), and in the second fit, the  $N_g = 0$  point is included. The parameter,  $\sigma_{abs}/\sigma_{pN}$ , resulting from the fit is  $0.23 \pm 0.09$  when neglecting the first data point in the fit, and  $0.13 \pm 0.05$  when including it. Taking the more conservative estimate of 0.23 and assuming  $\sigma_{pN}$  to be 30 mb, one obtains an absorption cross section,  $\sigma_{abs}$ , of  $6.9 \pm 2.7$  mb. At  $p = 2.5$  GeV/c, the mean measured momentum of the  $\bar{p}$  sample we detect, this is approximately 1/5 of the free annihilation cross section [12],  $\sigma_{ann}$ . The large discrepancy between  $\sigma_{abs}$ , as derived from our model, and  $\sigma_{ann}$  suggests a modification of the  $p - \bar{p}$  annihilation cross section within the nuclear medium. Figure 4 shows a very similar dependence of the mean  $\bar{\Lambda}$  yield on  $\nu$ . Fitting with the same function that was used for the  $\bar{p}$  yields, the extracted fit parameter is  $0.22 \pm 0.04$ . The effective absorption cross section is thus the same (within errors) for  $\bar{\Lambda}$  as for  $\bar{p}$ . This suggests an intermediate state that emerges from the nuclear medium as a  $\bar{p}$  or a  $\bar{\Lambda}$ .

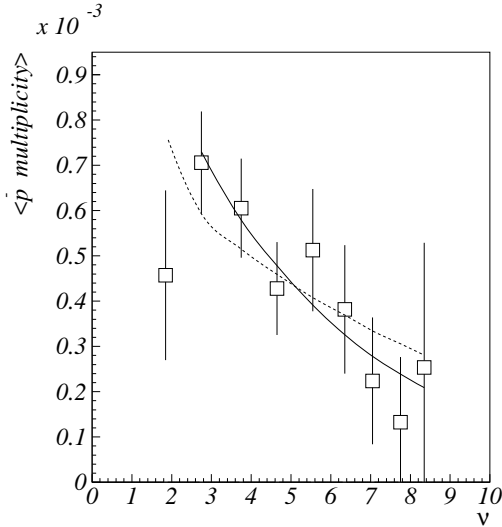


Figure 3. Dependence of mean  $\bar{p}$  yield on  $\nu$ . The solid line is the result of the fit neglecting the first point ( $N_g = 0$  bin), and the dashed line includes the first point.

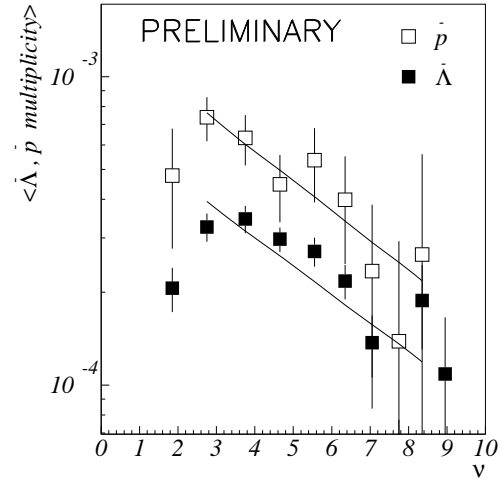


Figure 4. Dependence of mean  $\bar{p}$  yield and mean  $\bar{\Lambda}$  yield on  $\nu$  (semi-log scale). The open squares denote the  $\bar{p}$  data and the solid squares denote the  $\bar{\Lambda}$  data.

## 5. Conclusions

We have found that, at AGS energies, the  $\bar{p}$  yields dramatically increase with beam momentum and moderately decrease with increasing target size. We have found evidence that even at these beam momenta, near the production threshold of the  $\bar{p}$  and the  $\bar{\Lambda}$ , there is production beyond the first  $p+N$  collision for the  $\bar{\Lambda}$ , and a similar behavior for the  $\bar{p}$  is not excluded. Finally, the “effective” absorption cross section, calculated within the context of a simple model, is significantly reduced relative to the free  $p - \bar{p}$  annihilation cross section. The similarity between the calculated absorption cross sections for  $\bar{p}$  and  $\bar{\Lambda}$  may indicate the presence of a single intermediate state which leads to both final states.

## REFERENCES

1. O. Chamberlain *et al.*, *Il Nuovo Cimento* **3** (1956) 447.
2. T. Elioff *et al.*, *Phys. Rev.* **128** (1962) 869.
3. D. E. Dorfan *et al.*, *Phys. Rev. Lett.* **14** (1965) 995.
4. V. Koch, G.E. Brown and C.M. Ko, *Phys. Lett.* **B 265** (1991) 29.
5. C. Spieles *et al.*, *Phys. Rev.* **C 53** (1996) 2011.
6. Y. Pang *et al.*, *Phys. Rev. Lett.* **78** (1997) 3418.
7. M. Bleicher *et al.*, *Phys. Lett.* **B485** (2000) 133.
8. R. Rapp and E.V. Shuryak, *hep-ph/0008326* and *Phys. Rev. Lett.* **86** (2001) 2980.
9. U. Heinz *et al.*, *J. Phys. G:Nucl. Phys.* **12** (1986) 1237.
10. S. Gavin *et al.*, *Phys. Lett.* **B 234** (1990) 175.
11. I. Chemakin *et al.*, BNL E910 Collab., *Phys. Rev.* **C 60** (1999) 024902.
12. P. Koch and C.B. Dover, *Phys. Rev.* **C 40** (1989) 145.
13. H. Sako, E802 Collab., *Nucl. Phys.* **A 638** (1998) 427c.